UC San Diego
UC San Diego Previously Published Works

Title

In silico designed mRNA vaccines targeting CA-125 neoantigen in breast and ovarian cancer.

Permalink

https://escholarship.org/uc/item/22k903d4

Journal

Vaccine, 41(12)

Authors

Lu, Lingeng

Johnson, Caroline

Khan, Sajid

et al.

Publication Date

2023-03-17

DOI

10.1016/j.vaccine.2023.02.048

Peer reviewed

HHS Public Access
Author manuscript
Vaccine. Author manuscript; available in PMC 2024 March 17.

In silico designed mRNA vaccines targeting CA-125 neoantigen in breast and ovarian cancer

Lingeng Lu[1,2,*], **Wenxue Ma**[3], **Caroline H. Johnson**[2,4], **Sajid A. Khan**[2,6], **Melinda L. Irwin**[1,2], **Lajos Pusztai**[2,5]

[1.]Department of Chronic Disease Epidemiology, Yale School of Public Health, Yale University, New Haven, CT 06510, USA

[2.]Yale Cancer Center, Yale University, New Haven, CT 06510, USA

[3.]Department of Medicine, Moores Cancer Center and Sanford Stem Cell Clinical Center, University of California San Diego, La Jolla, CA 92093, USA

[4.]Department of Environmental Health Science, Yale School of Public Health, Yale University, New Haven, CT 06510, USA

[5.]Department of Medical Oncology, Yale School of Medicine, Yale University, New Haven, CT 06510, USA

[6.]Department of Surgery, Yale School of Medicine, Yale University, New Haven, CT 06510, USA

Abstract

Somatic mutation-derived neoantigens are associated with patient survival in breast and ovarian cancer. These neoantigens are targets for cancer, as shown by the implementation of neo-epitope peptides as cancer vaccines. The success of cost-effective multi-epitope mRNA vaccines against SARS-Cov-2 in the pandemic established a model for reverse vaccinology. In this study, we aimed to develop an in silico pipeline designing an mRNA vaccine of the CA-125 neoantigen against breast and ovarian cancer, respectively. Using immuno-bioinformatics tools, we predicted cytotoxic CD8+ T cell epitopes based on somatic mutation-driven neoantigens of CA-125 in breast or ovarian cancer, constructed a self-adjuvant mRNA vaccine with CD40L and MHC-I -targeting domain to enhance cross-presentation of neo-epitopes by dendritic cells. With an in silico ImmSim algorithm, we estimated the immune responses post-immunization, showing IFN-γ and CD8+ T cell response. The strategy described in this study may be scaled up and implemented to design precision multi-epitope mRNA vaccines by targeting multiple neoantigens.

*Corresponding author: Lingeng Lu, MD, PhD, Department of Chronic Disease Epidemiology, Yale School of Public Health, 60 College Street, New Haven, CT 06510, USA. Tel: 203-737-6812. lingeng.lu@yale.edu.

Conflict of Interests: We have no conflict of interest to declare.

Introduction

Antigens are a detonator of immune response in cancer immunotherapy. Two different types of antigens exist in human cancer: tumor-associated and tumor-specific antigens. Tumor-associated antigens are the proteins that are at elevated expression levels in tumor cells, but at relatively much lower levels in healthy cells. In contrast, tumor-specific antigens (also called neoantigens) exclusively exist in tumor cells and are derived from somatic mutations that alter amino acid sequences. After being presented by antigen-presenting cells (e.g., dendritic cells), the MHC-I-neoantigen peptide complex can prime and activate cytotoxic CD8+ T cells, eliciting immune responses and consequently eliminating tumor cells. *Ex vivo* co-culture experimental results have shown that neoantigen-pulsed dendritic cells can successfully induce co-cultured CD8+ T cells [1]. Clinical studies have also demonstrated that neoantigen levels are associated with overall survival in patients with malignancies, e.g., breast cancer, ovarian cancer and melanoma [2-5].

A positive association was also found between neoantigens and both T cell activation and checkpoint inhibitor responses across human cancers [6]. High mutation loads significantly improved immunotherapy efficacy in melanoma and lung cancer [7]. The expression level of *BRCA1,* a DNA damage repair-related gene, modified the effect of effector T cell activation score on patient survival in breast cancer [8]. These observations also indicate the involvement of neoantigens in immune response, given that neoantigen loads were highly correlated with mutation burdens [9]. Inefficient spontaneous immune recognition of mutations prompts the proof-of-concept of synthetic neoantigen vaccines for cancer immunotherapy. In a Lynch Syndrome mouse model, a neoantigen vaccine induced both cellular and humoral protective immunity with significant reduction of tumor burden and improved survival of colorectal cancer [10]. Two clinical studies with a relatively small sample size also showed a promising clinical outcome of individualized neoantigen vaccines. Synthetic individualized neoantigen peptides elicited neoantigen-specific CD8+ and CD4+ T cells, and some of the peptides significantly improved anti-PD-1 therapy efficacy in the vaccinated melanoma patients with either no recurrence within 25 months post-vaccination or complete tumor regression [11]. Similar results of synthetic personal neoantigen vaccines in a prime-boost schedule after radiotherapy were also observed in a phase I/Ib study on patients with glioblastoma [12], or in combination with PD-1 blockade on patients with other human cancers including non-small cell lung cancer, bladder cancer or melanoma [13].

The successful development of the SARS-Cov-2 mRNA vaccine has re-ignited enthusiasm for reverse vaccinology approaches, which starts from genomic sequences to the design of epitope vaccines using different bioinformatic tools. This approach substantially cut the efforts and costs needed for target vaccine discovery from bench to bedside. By implementing a RNA-based neoantigen approach, Sahin and colleagues [14] reported the

first clinical trial on precision neoantigen-derived mRNA vaccines that were designed and administrated to five patients with melanoma. Vaccine-induced T cell responses were observed in all patients, and two of them with metastatic disease had an improved progression-free survival. A complete response was found in one patient who received anti-PD-1 therapy after the vaccination. mRNA-based vaccines have intrinsic adjuvant activity [15], whereas neoantigen peptides-based vaccines thus far are administrated together with adjuvants (e.g., TLR3 agonist poly-ICLC).

Carbohydrate antigen 125 (CA-125, also known as MUC16) is an overexpressed protein in several human cancers including breast and ovarian cancers, and it is a biomarker clinically used for the diagnosis of breast and ovarian cancer, and monitoring the disease progression. It has been reported that CA-125 neoantigens and neoantigen-specific T cells were enriched in long-term survivors of pancreatic ductal adenocarcinoma (PDAC) [16]. Approximately 42-56% reduction in mortality was observed in melanoma patients with vs. without CA-125 mutations [17]. In gastric cancer, patients who had CA-125 mutations survived 20.2 months longer than those without the mutations [18]. In breast cancer, Li and colleagues also reported that neoantigen expression levels are positively associated with patient overall survival, and that CA-125 neoantigens are the most shared by these patients [2]. In this study, we aimed to design self-adjuvant neoantigen mRNA-based vaccines targeting CA-125 as an example in breast and ovarian cancer using in silico methods.

Materials and Methods

CA-125 neoantigen prediction

Somatic mutations in CA-125 were retrieved from a The Cancer Genome Atlas (TCGA) invasive breast carcinoma or ovarian cancer dataset at Genomic Data Commons (GDC) data portal (https://portal.gdc.cancer.gov) using an R package 'TCGAbiolinks' [19]. Only those single nucleotide mutations that change peptide sequences were included in this study for neoantigen prediction. As previously described elsewhere [20], NetMHCpan v4.0 was used to estimate the binding affinity between either mutated or corresponding wild-type peptides and HLA (MHC-I) alleles. The definition of the neoantigen in this study for further analyses is that the binding affinity (IC50) of the mutated peptide is less than 500 nM (IC50 < 500 nM), whereas the corresponding wild-type peptide has IC50 > 500 nM.

Cytotoxic CD8+ T cell (CTL) epitope prediction

Being a CD8+ T cell epitope, the peptides are required to be pre-processed by the cleavage system in antigen-presenting cells (APCs), followed by the transport system (TAP) to HLA molecules. The presented HLA-peptides complex is recognized by the T cell receptor (TCR) to activate CD8+ T cells. NetCTL v1.2 is an immunobioinformatics tool for CTL epitope prediction, which integrates proteasomal cleavage, TAP transport efficiency and MHC-I affinity. Twelve MHC-I supertypes (A1, A2, A3, A24, A26, B7, B8, B27, B39, B44, B59 and B62) are included in NetCTL v1.2 for 9-mer CTL epitope prediction on the neoantigens. A combined score was estimated in NetCTL, and 0.75 was selected as the cut-off value for epitope prediction. With the cut-off value of 0.75, the sensitivity and specificity for the CTL epitope prediction are 80% and 97%, respectively [21].

Neoantigen toxicity and allergenicity prediction

ToxinPred [22] and AllerTOP v2.0 [23] were applied to predict the toxicity and allergenicity of the neoantigens. Support Vector Machine Learning (SVM) (Swiss-Prot)-based method with the default parameters was chosen in ToxinPred. K nearest neighbors (kNN) was implemented in the AllerTOP v2.0, which utilizes E-descriptors, auto- and cross-covariance (ACC) transformation of amino acid sequences, to distinguish allergens from non-allergens.

Neoantigen antigenicity prediction

VaxiJen v2.0 [24] was performed to predict the antigenicity of neoantigens with a threshold value of 0.5. Only those neoantigens with the property of probable antigen epitopes were selected for the vaccine construction. The constructed peptide vaccine was further analyzed for antigenicity using both VaxiJen and ANTIGENpro [25].

T helper cell (Th) epitope and interferon-gamma (IFN-γ), interleukin (IL)-2, IL-4 and IL-10 epitope prediction

T helper cells (including Th-1 and Th-2) play important roles in healthy immune responses by releasing IFN-γ, IL-2, IL-4 and IL-10. The involvement of both IL-2 and IL-4 have been shown in the activation of CD8+ T cells. By binding MHC-II-peptide complex, T helper cells are activated to assist either CD8+ T cell-mediated immune response or B cell-mediated humoral antibody immune response. In cancer immunotherapy, CD8+ T cell-mediated response is a major approach to eliminate tumor cells. Thus, in this study, we used a previously reported virus-derived 15-mer Th cell epitope [26], which has been shown non-toxic and non-allergenic, but with antigenicity, IFN-γ, IL-4 and IL-10 inducibility using the tools of ToxinPred, AllerTOP v2.0, VaxiJen v2.0, IFNepitope [27], IL4Pred [28] and IL10Pred [29], respectively. We also performed IL-2 inducibility for the Th cell epitopes using IL2Pred [30].

Population coverage in breast cancer with CA-125 neoantigens

IEDB analysis resource (tools.iedb.org/population) was applied to estimate population coverage based on the MHC alleles for the CTL neoantigen epitopes and Th cell epitope.

Multi-epitope vaccine candidate sequence assembly

The neoantigens with highly antigenic, non-toxic and non-allergenic epitopes were selected to assemble the candidate vaccine targeting CA-125 in either breast or ovarian cancer. Generally, after the muscle injection, the mRNA vaccine is taken up into muscle cells where the corresponding peptides are produced. The synthesized peptides are required to be secreted and then are taken up by antigen-presenting cells (APCs), e.g., dendritic cells and macrophages, to further elicit immune response. Thus, in the vaccine design we added three additional elements. One is a signal peptide, which can direct the synthesized peptides to be secreted out of the cells. We used SignalP [31] to predict the secretory signal peptide that is transported by the Sec translocon and cleaved by Signal Peptidase I based on tissue plasminogen activator (tPA-SP, GeneBank accession no. E02360, or UniProt ID: P00750). It has been shown that a modification of 22P/A substitution in the signal peptide of tPA-SP leads to enhanced expression and secretion of the target protein [32]. The second one is a

ligand of CD40 (CD40L, UniProt ID: P29965), which acts as an adjuvant to enhance the uptake of the synthesized peptides via the engagement of CD40L and CD40 receptor on APCs [33, 34]. The third one is MHC-I-targeting domain (MITD), which is able to direct the traffic of synthesized CTL epitopes to MHC-I compartment of endoplasmic reticulum [35]. GPGPG linkers were used to link CD40L and Th cell epitopes, and AAY linkers were for combining intra-CTL epitopes and Th cell epitopes. In addition, at the end of 5', 5'-m7G cap and beta globin 5'-UTR, and alpha globin 3'-UTR and 120-150 bp poly(A) tail were added to stabilize mRNAs [36].

The putative vaccine construct was then examined for allergenicity, and toxicity as described above. The physicochemical properties were evaluated using Expasy Protparam (https://web.expasy.org/protparam), which includes the molecular weight, estimated half-life, instability index, aliphatic index and grand average of hydropathicity (GRAVY).

Codon optimization

The differential usage of synonymous codons exists in cells, which depends on the abundance of their corresponding tRNAs. Codon optimization for vaccine mRNA aims to improve translation elongation efficiency and thereby decrease the copies of vaccine mRNA required. The Java Codon Adaptation (JCat) tool (www.jcat.de) was used to optimize codons for the candidate vaccine mRNA. The Kozak sequence containing the start codon site (GCCACC**AUG**, where **AUG** is the start codon) is required, which can enhance translation initiation [36].

In silico simulation of immune response

C-ImmSim is an algorithm simulating immune response in silico, which combines position-specific scoring matrix (PSSM) and machine learning to predict the immune response to the antigen epitopes [37]. We performed in silico simulation C-ImmSim to predict the immune response against the putative CA-125 neoantigen mRNA vaccine. The parameters for the algorithm simulation were set as: the simulation volume 10, simulation steps 100, one injection of vaccine without LPS, 100 adjuvant, and 1000 antigen.

Results

CA-125 neoantigens with CTL epitopes in either breast or ovarian cancer

With the criteria of neoantigen, we found 51 CA-125 peptides with somatic mutations in breast cancer. All these peptides had an MHC-I molecule binding affinity less than 500 nM for the mutated peptides, while greater than 500 nM for the wild-type peptides. None of the mutated peptides showed toxicity, and 22 mutated peptides were non-allergens. Of 51 CA-125 mutated peptides, 39 were predicted containing CTL epitopes for 12 MHC-I supertypes, and 23 were predicted as an antigen with an antigenicity score greater than 0.5 (Table 1). Taken together, 6 unique mutated peptides meeting all criteria in breast cancer (CTL neoantigen epitope, nontoxin, non-allergen, and antigenicity) were selected for CTL epitope vaccine construction (Table 2). Their corresponding predicted MHC-I binding alleles (percentile rank   2) are also shown in Table 2.

Similarly, in ovarian cancer, we found 3 unique mutated peptides meeting all criteria, whose corresponding predicted MHC-I binding alleles (percentile rank   2) are shown in Table 2.

Th cell epitope—The epitope (DLPIGINITRFQTLL) was previously reported as a Th cell epitope with a predicted inducibility of IFN-γ, IL-4 and IL-10. It was also predicted as an IL-2 inducer scoring 0.69, which is greater than the threshold of 0.5. The corresponding predicted MHC-II binding alleles are also shown in Table 2.

Population coverage of CA-125 neoantigen CTL epitopes in breast cancer patients

Six putative CA-125 neoantigen CTL epitopes with their corresponding MHC-I binding alleles, and Th cell epitope with its corresponding MHC-II binding alleles were used for population coverage estimation (Table 2). The coverage of 91.39% breast cancer patients with CA-125 neoantigens was found worldwide, and 99.22% in Europe, and 99.78% in North America. If count MHC-I binding alleles of the CTL epitopes only, the coverage was 71.52% worldwide, 80.58% in Europe, and 70.16% in North America (Figure 1).

Similarly, the coverage was also estimated based on 3 putative CA-125 neoantigen CTL epitopes in ovarian cancer. The coverages were 97.19% for ovarian cancer patients with CA-125 neoantigens worldwide, 99.93% in Europe, and 99.95% in North America, respectively, when including MHC-I and II epitopes. If considering MHC-I binding alleles of the CTL epitopes only, the coverages were 68.05% worldwide, 75.92% in Europe, and 63.0% in North America (data not shown).

CA-125 neoantigen vaccine assembly

The final entire construct of the CA-125 neoantigen vaccine for breast cancer is assembled as the follows in the order from the N- to C-terminal:

5'm7G Cap – 5'-UTR of β-globin – GCCACC**AUG** (Kozak Sequence) – MDAMKRGLCCVLLLCGAVFVSPS (t-PA secretary signal peptide) – HIS tag (GTGGGGSHHHHHHGGMASMTGGQQQQMGGGGGSSR) – CD40L sequence (aa 116-261 extracellular domain) (as adjuvant) – GPGPG – Th cell epitope (DLPIGINITRFQTLL) – AAY (linker) – VVTGSSATL – AAY – SLTESTHHL – AAY – YVGTTGSAF – AAY – IPGPAHSTM -AAY – SATTEVSMTK – AAY – KVLDTSSEPK – AAY – MITD sequence – Stop codon – α-globin 3'-UTR – poly (A) tail.

The putative generated protein (in vitro transcription, IVT) and its multiple neoepitope peptides were non-toxic and non-allergenic. The total number of amino acids is 550 with molecular weight of 60712.87. Total number of negative charged residues (Asp + Glu) is 51, and 55 positively charged residues (Arg + Lys). The estimated half-life is 30 hours in mammalian reticulocytes (in vitro). The Aliphatic index is 77.35, and GRAVY is –0.349. Instability index is 48.43 (Table 3).

After the codon optimization in human cells, the length of 1.65 kb mRNA sequence (which excludes 5'- and 3'-UTR sequence), contains 66.66% GC, and the codon optimization index (CAI) value was predicted 0.96.

Similarly, the construct of the CA-125 neoantigen vaccine for ovarian cancer is assembled as

5'm7G Cap – 5'-UTR of β-globin – GCCACC**AUG** (Kozak Sequence) – MDAMKRGLCCVLLLCGAVFVSPS (t-PA secretary signal peptide) – HIS tag (GTGGGGSHHHHHHGGMASMTGGQQQQMGGGGGSSR) – CD40L sequence (aa 116-261 extracellular domain) (as adjuvant) – GPGPG – Th cell epitope (DLPIGINITRFQTLL) – AAY (linker) –GAATGMNAI– AAY – RRNPSFGTLY – AAY – GTSSSGHESTY –AAY – MITD sequence – Stop codon – α-globin 3'-UTR – poly(A) tail.

The putative generated protein (IVT) and its multiple neoepitope peptides were non-toxic and non-allergenic. The total number of amino acids is 510 with molecular weight of 57150.79. Total number of negative charged residues (Asp + Glu) is 48, and 57 positively charged residues (Arg + Lys). The estimated half-life is 30 hours in mammalian reticulocytes (in vitro). The Aliphatic index is 76.16, and GRAVY is −0.412. Instability index is 51.52 (Table 3). After the codon optimization in human cells, the length of 1.545 kb mRNA sequence with the exclusion of 5'- and 3'-UTR sequence contains 66.54% GC, and CAI value was predicted 0.96.

Simulated immune response against CA-125 neoantigen vaccine

Using C-ImmSim algorithm, we simulated the immune response to the vaccine. With one dose stimulation, it was estimated that the number of Th1 cells but neither Th-2 nor Th-17 increased remarkably, reaching approximately 50,000 cells/mm^3 and accounting for approximately 80% of T helper cells 5 days of post-immunization (Figure 2A). The number of T helper cells at both active and resting states increased post-immunization, and remained relatively stable approximately for one month. Duplicating Th cells reached the maximum at day 5 post-immunization (Figure 2B). Active cytotoxic CD8+ T cells increased up to approximately 1000 cells/mm^3, while resting CD8+ T cells declined approximately from 1100 to 200 cells/mm^3 post-immunization. No anergic cytotoxic T cells appeared (Figure 2C). The number of dendritic cells with internalized antigens appeared within 5 days of post-immunization, and presenting cells increased post-immunization, although the levels remained relatively much lower compared to total and resting dendritic cells (Figure 2D). Similarly, a peak was observed for macrophage either with internalized antigens or as presenting cells within 5 and 10 days post-immunization, respectively. The number of resting macrophages declined at the first 2 days post-immunization and then gradually increased as active state (Figure 2E). A dramatic increase in IFN-γ was observed, and reached the maximum (450,000 ng/ml) around day 15. The cytokine IL-2 reached the maximum level (350,000 ng/ml) at approximately day 8. TGF-beta, IL-10 and IL-12 increased slightly (less than 100,000 ng/ml) (Figure 2F).

Similarly, with one dose stimulation of ovarian cancer CA-125 neoantigen, the number of Th1 cells but neither Th-2 nor Th-17 increased remarkably, reaching approximately 70,000 cells/mm^3 and accounting for over 80% of T helper cells 7 days of post-immunization (Figure 3A). The number of T helper cells at both active and resting states increased post-immunization, and remained relatively stable approximately for one month. Duplicating Th cells reached the maximum at day 7 post-immunization (Figure 3B). Active cytotoxic

CD8+ T cells increased up to over 400 cells/mm^3, while resting CD8+ T cells declined approximately from 1100 to about 700 cells/mm^3 post-immunization. No anergic cytotoxic T cells appeared (Figure 3C). The increased number of dendritic cells with internalized antigens appeared within 6 days of post-immunization, and presenting-2 dendritic within 10 days, and active dendritic increased post-immunization and last about one month, although the levels remained relatively much lower compared to total and resting dendritic cells (Figure 3D). Again, a peak was observed for macrophage either with internalized antigens or as presenting cells within 8 and 13 days post-immunization, respectively. The number of resting macrophages declined at the first 2 days post-immunization and then gradually increased as active state (Figure 3E). A dramatic increase in IFN-γ was observed, and reached the maximum (450,000 ng/ml) around day 12. The cytokine IL-2 reached the maximum level (470,000 ng/ml) at approximately day 8. TGF-beta, IL-10 and IL-12 increased slightly (TGF-beta < 200,000 ng/ml, IL-10 and IL-12< 100,000 ng/ml) (Figure 3F).

Discussion

In this study, we present strategies to design self-adjuvant neoantigen mRNA-based vaccines targeting CA-125 in silico, using both breast and ovarian cancer to demonstrate this model. We first determined neoantigens based on non-synonymous somatic mutations for CTL epitope prediction. However, we did not include B cell neoantigen epitopes. Tumor-specific cytotoxic CD8+ T cells are in no doubt killers of tumor cells, playing a dominant role in cancer immunotherapy. Activated effector CD8+ T cells significantly improve patient survival, and the goal of both immune checkpoint inhibitors and cancer vaccines is to reinvigorate or induce tumor-specific cytotoxic CD8+ T cells. In contrast, the role of B cells is still controversial in cancer progression. Significant B cell populations exist in human solid cancer, indicating that B cells may influence the tumor microenvironment by orchestrating with other resident cells. High B cells in untreated patients with node-negative breast cancer were significantly associated with better metastasis-free survival [38] and ovarian cancer [39]. However, B cells have also been shown to drive tumor progression in different ways, e.g., antibody-mediated immune suppression, B cell-secreted factors, and cytokines. Circulating Antigen-antibody complexes are deposited in premalignant tissue, Fcγ receptors on resident and infiltrating myeloid cells are activated, fostering cancer development and progression [40]. The activation of complement pathway, on the other hand, also triggers pro-angiogenic, pro-metastatic and invasive program, and inhibits cytotoxic CD8+ T cells [41]. Regulatory B cells, a heterogeneous population, can produce a variety of immunosuppressive cytokines (e.g., IL-10 and TGF-β) that inhibit CD8+ T cells, CD4+ T helper cells and NK cells, consequently promoting tumor growth and progression [41-43].

Dendritic cells (DCs), professional antigen-presenting cells (APCs), function as instructors in immune response by presenting captured antigens in the form of MHC-I- or II-peptide complexes. The MHC-I- or II-peptide complexes then prime and activate T and B cells. CD40 receptors are expressed on DCs, and CD40L, a ligand of CD40, has been shown to function as an adjuvant that increases antigen uptake and processing for cross-presentation, promoting DCs maturation and activating T cells. The combination of CD40L and IFN-γ

is necessary in inducing DCs to secrete IL-12, the cytokine for polarizing Th-1 cells. In the putative synthesized peptides, we included an epitope for T helper cells, which was derived from a virus protein rather than human protein, and contains a predicted motif to induce IFN-γ, IL-4, IL-10 and IL-2. Besides IFN-γ, IFN-α has also been shown with an ability to enhance CD40L-mediated maturation and activation of DCs. The activated DCs with CD40L, in turn, produce numerous cytokines including IL-12, IL-1β, IL-1α and IFN-γ, and these cytokines orchestrate together to stimulate CD8+ T cell development. One of the reasons why we include a foreign peptide rather than neoantigen-derived self-peptide is that the foreign antigen may elicit stronger immune response and cytokine productions. Another reason is that the role of B cells in the cancer progression was still controversial, given that neoantigen-based Th epitopes may also act as B epitopes and elicit neoantigen-specific antibodies. However, such a foreign antigen as the Th epitope (but this can be a strategy to design a vaccine for virus-caused or -related tumors) also has its limitation that the tumor-specific Th cells may not be elicited. For other types of human cancer, in which if B cells have beneficial effects on patient survival, neoantigen-based Th epitopes, which may also act as B cell epitopes and elicit antibodies against the neoantigens-bearing tumor, are recommended to replace the foreign antigen-based ones. In this regard, neoantigen-specific Th cells can be elicited.

The density of surface epitope/MHC-I complexes on DCs is another determinant of immune response. Low dense complexes not only lead to reduced antigen-specific CD8+ T cell memory size and weak immune response, but also favor the polarization of CD4+ Th-2 cell response. Besides an antigen itself, the processing and presentation of antigens in DCs also affect the surface density of MHC/peptide complexes. As low as 1 peptide/10,000 degraded molecules are presented in MHC-I/peptide complexes [35]. MHC-I molecules travel through the endocytic pathway as MHC-II antigen processing and presentation, from endoplasmic reticulum, Golgi apparatus, early and late endosomes and lysosomes. CD4+ T helper epitopes are loaded onto MHC-II in the late endosome, whereas processed peptides are loaded onto MHC-I in endoplasmic reticulum. A previous study has shown that MHC-I molecule trafficking domain (MITD, aa 308-362) could efficiently improve the cross-presentation of the MITD-antigen fusion protein for both MHC-I and II molecules, significantly eliciting antigen-specific CD4+ and CD8+ T cells by increasing the surface density of peptide/MHC complexes [35]. In cancer mouse models, mice benefit from the MITD-tagged antigen-specific vaccine with significantly longer survival [35].

A recent clinical trial reported no objective responses, in which four patients with metastatic gastrointestinal cancer were treated with KRAS[G12D] neoantigen mRNA vaccine, and the vaccine induced the neoepitope-specific T cells [44]. One possibility of this failure, per the study authors, stems from the pre-treatment of patients with tumor-infiltrating lymphocytes (TIL), who had undergone conditional lymphodepletion with cyclophosphamide and fludarabine in compliance to the TIL protocol. Other possibilities included TIL exhaustion and lack of antigenic epitopes in the vaccine backbone or other individual factors. This result suggests that TIL is another efficient barrier of neoantigen vaccines. Several strategies have been proposed to overcome this hurdle, e.g., oncolytic virus, and attenuated mycobacterium [45, 46]. The lytic tumor cells release tumor antigens together with the virus-associated danger signaling not only drive antigen presentation in tumor-draining lymph nodes, but

also induce TIL[45, 46]. Mycobacterium, an intracellular pathogen, can induce chemokines and cytokines that recruit lymphocytes. Mycobacterium-coated tumor vaccine increased the abundance of antigen-specific CD8+ T cells. Different attenuated *Salmonella* Typhimurium strains have been made, which favor to grow in different types of human solid cancer and inhibit the tumor growth [47]. For example, aromatase A-deleted (aroA) S. Typhimurium is auxotrophic for aromatic amino acids, which are enriched in tumor microenvironment that facilitates the growth colonization of aroA-*S.* Typhimurium compared with the normal tissues [48]. The colonized and grown attenuated *S.* Typhimurium could significantly reduce the tumor burden, and alter transcriptional and metabolic landscape of tumors in colorectal cancer [48]. The downregulated genes include those involved in DNA damage response and repair, epithelial-mesenchymal transition in the attenuated *S.* Typhimurium treatment. The elevated amino acids and tricarboxylic acid (TCA) cycle intermediates in tumor tissues declined after the attenuated *S.* Typhimurium treatment. Survival of mice with tumors was also prolonged [48]. Collagenase-expressing *S.* Typhimurium led to the reduction of an immunosuppressive environment in pancreatic ductal carcinoma by degrading intra-tumoral collagens, fostering a favorable microenvironment for immunotherapy [49]. Another recent study showed that attenuated *S.* Typhimurium that carries neoantigens invaded and grew in tumors, consequently suppressing tumor growth and prolonged survival with a relative increase of CD4+ and CD8+ T cells in tumor mouse models [50]. In this study, the designed mRNA vaccine cannot only be subcutaneously injected into patients, but can also be modified for expression of neoantigen fused protein in attenuated *S.* Typhimurium by optimizing the codons for the CA-125 neoantigen vaccine assembly. This modified scheme will allow to orally gavage the attenuated S. Typhimurium-carrying neoantigens for gastrointestinal cancer or intravenous administrate the bacterium for other types of solid cancer. The attenuated *S.* Typhimurium-mediated approach takes advantage of the ability of attenuated auxotrophic *S.* Typhimurium to selectively grow in tumor tissues, and induce "hot" tumors.

The application of neoantigen-based vaccines may promote the epitope spreading of T cell responses to those neoantigens that are not contained in the injected vaccines. This epitope spreading might associate with improved progression-free survival (HR=0.23, 95% CI: 0.06-0.83) in the group of patients with either urothelial carcinoma, non-small cell lung cancer (NSCLC) and melanoma [13]. However, the application of the neoantigen mRNA vaccine in clinical settings is still challenging. *Ex vivo* experiments of circulating T cells showed that 77% of patients responded to a median of 2.6 neoantigens, and the frequency of epitope-specific CD8+ T cells in peripheral blood was about 5% [51]. In another study enrolling 14 patients with TNBC, all individuals had vaccine-induced CD8+ and/or CD4+ T cell responses to 1 to 10 of the vaccine neoepitopes, and up to 10.3% peripheral CD8 T cells were specific against neoepitopes [52]. The overall of object response rate (ORRs) was 8% (range from 4% to 30%) in the cohorts of patients with triple negative breast cancer, urothelial carcinoma, RCC, melanoma or NSCLC [51]. A recent randomized phase 2b clinical trial enrolling 157 patients with stage III/IV melanoma showed that the risk of recurrence or death was reduced by 44% (HR=0.56, 95% CI: 0.31-1.08, one-side p value =0.0266) in the group of the mRNA-4157/V940 vaccine containing 34 neoantigens in combination with KEYTRUDA compared with KEYTRUDA alone [53].

In summary, in this study we used CA-125 as an example to perform an in silico design of a multi-epitope mRNA self-adjuvant vaccine targeting CA-125 neoantigen in either breast or ovarian cancer using immuno-bioinformatics tools, and systemically described the strategy in the design. This mRNA-based vaccine construct can be transformed into an expression vector, and expressed in attenuated *S. Typhimurium* by taking advantage of the bacterial auxotrophic growth in tumor tissues. Expressed CD40L-neoantigen epitopes-MITD fused proteins are cross-presented by DCs, and activate neoantigen-specific CD8+ T cells to kill the tumor. This pipeline can be scaled up and generalized to design multi-epitopes precision vaccines by targeting multiple neoantigens. This is a cost-effective approach to design a tumor vaccine for validation of *in vitro* and *in vivo* preclinical studies, and then clinical application.

Acknowledgements:

References:

[1]. Morisaki T, Kubo M, Umebayashi M, Yew PY, Yoshimura S, Park JH, et al. Neoantigens elicit T cell responses in breast cancer. Sci Rep. 2021;11:13590. [PubMed: 34193879]

[2]. Li W, Amei A, Bui F, Norouzifar S, Lu L, Wang Z. Impact of Neoantigen Expression and T-Cell Activation on Breast Cancer Survival. Cancers (Basel). 2021;13:2879. [PubMed: 34207556]

[3]. Strickland KC, Howitt BE, Shukla SA, Rodig S, Ritterhouse LL, Liu JF, et al. Association and prognostic significance of BRCA1/2-mutation status with neoantigen load, number of tumor-infiltrating lymphocytes and expression of PD-1/PD-L1 in high grade serous ovarian cancer. Oncotarget. 2016;7:13587–98. [PubMed: 26871470]

[4]. Lauss M, Donia M, Harbst K, Andersen R, Mitra S, Rosengren F, et al. Mutational and putative neoantigen load predict clinical benefit of adoptive T cell therapy in melanoma. Nat Commun. 2017;8:1738. [PubMed: 29170503]

[5]. Ren Y, Cherukuri Y, Wickland DP, Sarangi V, Tian S, Carter JM, et al. HLA class-I and class-II restricted neoantigen loads predict overall survival in breast cancer. Oncoimmunology. 2020;9:1744947. [PubMed: 32523802]

[6]. Turajlic S, Litchfield K, Xu H, Rosenthal R, McGranahan N, Reading JL, et al. Insertion-and-deletion-derived tumour-specific neoantigens and the immunogenic phenotype: a pan-cancer analysis. Lancet Oncol. 2017;18:1009–21. [PubMed: 28694034]

[7]. Roszik J, Haydu LE, Hess KR, Oba J, Joon AY, Siroy AE, et al. Novel algorithmic approach predicts tumor mutation load and correlates with immunotherapy clinical outcomes using a defined gene mutation set. BMC Med. 2016;14:168. [PubMed: 27776519]

[8]. Lu L, Huang H, Zhou J, Ma W, Mackay S, Wang Z. BRCA1 mRNA expression modifies the effect of T cell activation score on patient survival in breast cancer. BMC Cancer. 2019;19:387. [PubMed: 31023256]

[9]. Narang P, Chen M, Sharma AA, Anderson KS, Wilson MA. The neoepitope landscape of breast cancer: implications for immunotherapy. BMC Cancer. 2019;19:200. [PubMed: 30832597]

[10]. Gebert J, Gelincik O, Oezcan-Wahlbrink M, Marshall JD, Hernandez-Sanchez A, Urban K, et al. Recurrent Frameshift Neoantigen Vaccine Elicits Protective Immunity With Reduced Tumor Burden and Improved Overall Survival in a Lynch Syndrome Mouse Model. Gastroenterology. 2021;161:1288–302 e13. [PubMed: 34224739]

[11]. Ott PA, Hu Z, Keskin DB, Shukla SA, Sun J, Bozym DJ, et al. An immunogenic personal neoantigen vaccine for patients with melanoma. Nature. 2017;547:217–21. [PubMed: 28678778]

[12]. Keskin DB, Anandappa AJ, Sun J, Tirosh I, Mathewson ND, Li S, et al. Neoantigen vaccine generates intratumoral T cell responses in phase Ib glioblastoma trial. Nature. 2019;565:234–9. [PubMed: 30568305]

[13]. Ott PA, Hu-Lieskovan S, Chmielowski B, Govindan R, Naing A, Bhardwaj N, et al. A Phase Ib Trial of Personalized Neoantigen Therapy Plus Anti-PD-1 in Patients with Advanced Melanoma, Non-small Cell Lung Cancer, or Bladder Cancer. Cell. 2020;183:347–62 e24. [PubMed: 33064988]

[14]. Sahin U, Derhovanessian E, Miller M, Kloke BP, Simon P, Lower M, et al. Personalized RNA mutanome vaccines mobilize poly-specific therapeutic immunity against cancer. Nature. 2017;547:222–6. [PubMed: 28678784]

[15]. Kreiter S, Selmi A, Diken M, Koslowski M, Britten CM, Huber C, et al. Intranodal vaccination with naked antigen-encoding RNA elicits potent prophylactic and therapeutic antitumoral immunity. Cancer Res. 2010;70:9031–40. [PubMed: 21045153]

[16]. Balachandran VP, Luksza M, Zhao JN, Makarov V, Moral JA, Remark R, et al. Identification of unique neoantigen qualities in long-term survivors of pancreatic cancer. Nature. 2017;551:512–6. [PubMed: 29132146]

[17]. Wang Q, Yang Y, Yang M, Li X, Chen K. High mutation load, immune-activated microenvironment, favorable outcome, and better immunotherapeutic efficacy in melanoma patients harboring MUC16/CA125 mutations. Aging (Albany NY). 2020;12:10827–43. [PubMed: 32491995]

[18]. Li X, Pasche B, Zhang W, Chen K. Association of MUC16 Mutation With Tumor Mutation Load and Outcomes in Patients With Gastric Cancer. JAMA Oncol. 2018;4:1691–8. [PubMed: 30098163]

[19]. Colaprico A, Silva TC, Olsen C, Garofano L, Cava C, Garolini D, et al. TCGAbiolinks: an R/Bioconductor package for integrative analysis of TCGA data. Nucleic Acids Res. 2016;44:e71. [PubMed: 26704973]

[20]. Wu J, Zhao W, Zhou B, Su Z, Gu X, Zhou Z, et al. TSNAdb: A Database for Tumor-specific Neoantigens from Immunogenomics Data Analysis. Genomics Proteomics Bioinformatics. 2018;16:276–82. [PubMed: 30223042]

[21]. Andreatta M, Nielsen M. Gapped sequence alignment using artificial neural networks: application to the MHC class I system. Bioinformatics. 2016;32:511–7. [PubMed: 26515819]

[22]. Gupta S, Kapoor P, Chaudhary K, Gautam A, Kumar R, Raghava GP. Peptide toxicity prediction. Methods Mol Biol. 2015;1268:143–57. [PubMed: 25555724]

[23]. Dimitrov I, Bangov I, Flower DR, Doytchinova I. AllerTOP v.2--a server for in silico prediction of allergens. J Mol Model. 2014;20:2278. [PubMed: 24878803]

[24]. Doytchinova IA, Flower DR. VaxiJen: a server for prediction of protective antigens, tumour antigens and subunit vaccines. BMC Bioinformatics. 2007;8:4. [PubMed: 17207271]

[25]. Magnan CN, Zeller M, Kayala MA, Vigil A, Randall A, Felgner PL, et al. High-throughput prediction of protein antigenicity using protein microarray data. Bioinformatics. 2010;26:2936–43. [PubMed: 20934990]

[26]. Ahammad I, Lira SS. Designing a novel mRNA vaccine against SARS-CoV-2: An immunoinformatics approach. Int J Biol Macromol. 2020;162:820–37. [PubMed: 32599237]

[27]. Dhanda SK, Vir P, Raghava GP. Designing of interferon-gamma inducing MHC class-II binders. Biol Direct. 2013;8:30. [PubMed: 24304645]

[28]. Dhanda SK, Gupta S, Vir P, Raghava GP. Prediction of IL4 inducing peptides. Clin Dev Immunol. 2013;2013:263952. [PubMed: 24489573]

[29]. Nagpal G, Usmani SS, Dhanda SK, Kaur H, Singh S, Sharma M, et al. Computer-aided designing of immunosuppressive peptides based on IL-10 inducing potential. Sci Rep. 2017;7:42851. [PubMed: 28211521]

[30]. Lathwal A, Kumar R, Kaur D, Radhava GPS. In silico model for predicting IL-2 inducing peptides in human. bioRxiv. 2021.

[31]. Almagro Armenteros JJ, Tsirigos KD, Sonderby CK, Petersen TN, Winther O, Brunak S, et al. SignalP 5.0 improves signal peptide predictions using deep neural networks. Nat Biotechnol. 2019;37:420–3. [PubMed: 30778233]

[32]. Wang JY, Song WT, Li Y, Chen WJ, Yang D, Zhong GC, et al. Improved expression of secretory and trimeric proteins in mammalian cells via the introduction of a new trimer motif and a mutant of the tPA signal sequence. Appl Microbiol Biotechnol. 2011;91:731–40. [PubMed: 21556920]

[33]. Palumbo RN, Nagarajan L, Wang C. Recombinant monomeric CD40 ligand for delivering polymer particles to dendritic cells. Biotechnol Prog. 2011;27:830–7. [PubMed: 21538973]

[34]. Kwa S, Lai L, Gangadhara S, Siddiqui M, Pillai VB, Labranche C, et al. CD40L-adjuvanted DNA/modified vaccinia virus Ankara simian immunodeficiency virus SIV239 vaccine enhances SIV-specific humoral and cellular immunity and improves protection against a heterologous SIVE660 mucosal challenge. J Virol. 2014;88:9579–89. [PubMed: 24920805]

[35]. Kreiter S, Selmi A, Diken M, Sebastian M, Osterloh P, Schild H, et al. Increased antigen presentation efficiency by coupling antigens to MHC class I trafficking signals. J Immunol. 2008;180:309–18. [PubMed: 18097032]

[36]. Xia X. Detailed Dissection and Critical Evaluation of the Pfizer/BioNTech and Moderna mRNA Vaccines. Vaccines (Basel). 2021;9:734. [PubMed: 34358150]

[37]. Rapin N, Lund O, Bernaschi M, Castiglione F. Computational immunology meets bioinformatics: the use of prediction tools for molecular binding in the simulation of the immune system. PLoS One. 2010;5:e9862. [PubMed: 20419125]

[38]. Schmidt M, Bohm D, von Torne C, Steiner E, Puhl A, Pilch H, et al. The humoral immune system has a key prognostic impact in node-negative breast cancer. Cancer Res. 2008;68:5405–13. [PubMed: 18593943]

[39]. Milne K, Kobel M, Kalloger SE, Barnes RO, Gao D, Gilks CB, et al. Systematic analysis of immune infiltrates in high-grade serous ovarian cancer reveals CD20, FoxP3 and TIA-1 as positive prognostic factors. PLoS One. 2009;4:e6412. [PubMed: 19641607]

[40]. Andreu P, Johansson M, Affara NI, Pucci F, Tan T, Junankar S, et al. FcRgamma activation regulates inflammation-associated squamous carcinogenesis. Cancer Cell. 2010;17:121–34. [PubMed: 20138013]

[41]. Gunderson AJ, Coussens LM. B cells and their mediators as targets for therapy in solid tumors. Exp Cell Res. 2013;319:1644–9. [PubMed: 23499742]

[42]. Gavrielatou N, Vathiotis I, Economopoulou P, Psyrri A. The Role of B Cells in Head and Neck Cancer. Cancers (Basel). 2021;13:5383. [PubMed: 34771546]

[43]. Lund FE. Cytokine-producing B lymphocytes-key regulators of immunity. Curr Opin Immunol. 2008;20:332–8. [PubMed: 18417336]

[44]. Cafri G, Gartner JJ, Zaks T, Hopson K, Levin N, Paria BC, et al. mRNA vaccine-induced neoantigen-specific T cell immunity in patients with gastrointestinal cancer. J Clin Invest. 2020;130:5976–88. [PubMed: 33016924]

[45]. Ylosmaki E, Malorzo C, Capasso C, Honkasalo O, Fusciello M, Martins B, et al. Personalized Cancer Vaccine Platform for Clinically Relevant Oncolytic Enveloped Viruses. Mol Ther. 2018;26:2315–25. [PubMed: 30005865]

[46]. Das K, Belnoue E, Rossi M, Hofer T, Danklmaier S, Nolden T, et al. A modular self-adjuvanting cancer vaccine combined with an oncolytic vaccine induces potent antitumor immunity. Nat Commun. 2021;12:5195. [PubMed: 34465781]

[47]. Mi Z, Feng ZC, Li C, Yang X, Ma MT, Rong PF. Salmonella-Mediated Cancer Therapy: An Innovative Therapeutic Strategy. J Cancer. 2019;10:4765–76. [PubMed: 31598148]

[48]. Mackie GM, Copland A, Takahashi M, Nakanishi Y, Everard I, Kato T, et al. Bacterial cancer therapy in autochthonous colorectal cancer affects tumor growth and metabolic landscape. JCI Insight. 2021;6:e139900. [PubMed: 34710062]

[49]. Ebelt ND, Zamloot V, Zuniga E, Passi KB, Sobocinski LJ, Young CA, et al. Collagenase-Expressing Salmonella Targets Major Collagens in Pancreatic Cancer Leading to Reductions in Immunosuppressive Subsets and Tumor Growth. Cancers (Basel). 2021;13:3565. [PubMed: 34298778]

[50]. Hyun J, Jun S, Lim H, Cho H, You SH, Ha SJ, et al. Engineered Attenuated Salmonella typhimurium Expressing Neoantigen Has Anticancer Effects. ACS Synth Biol. 2021;10:2478–87. [PubMed: 34525796]

[51]. Lopez JS, Camidge R, Iafolla M, Rottey S, Schuler M, Hellmann M, et al. A phase Ib study to evalute R07198457, an indivdidualized neoantigen sepcific immunotherapy (iNesST), in combination with atezolizumab in patients with locally advanced or metastatic solid tumors. Cancer Res. 2020;80:1.

[52]. Schmidt M, Vogler I, Derhovanessian E, Omokoko T, Godehardt E, Attig S, et al. 88MO T-cell responses induced by an individualized neoantigen specific immune therapy in post(neo)adjuvant patients with triple negative breast cancer. Annal Oncol. 2020;31:1.

[53]. Moderna. Modern and MErck announce mRNA-4157/V940, an investigational personalized mRNA cancer vaccine, in combinatiojn with KEYTRUDA(R)(pembrolizumab), met primary efficacy endopoint in phase 2B keynote-942 trial. 2022.
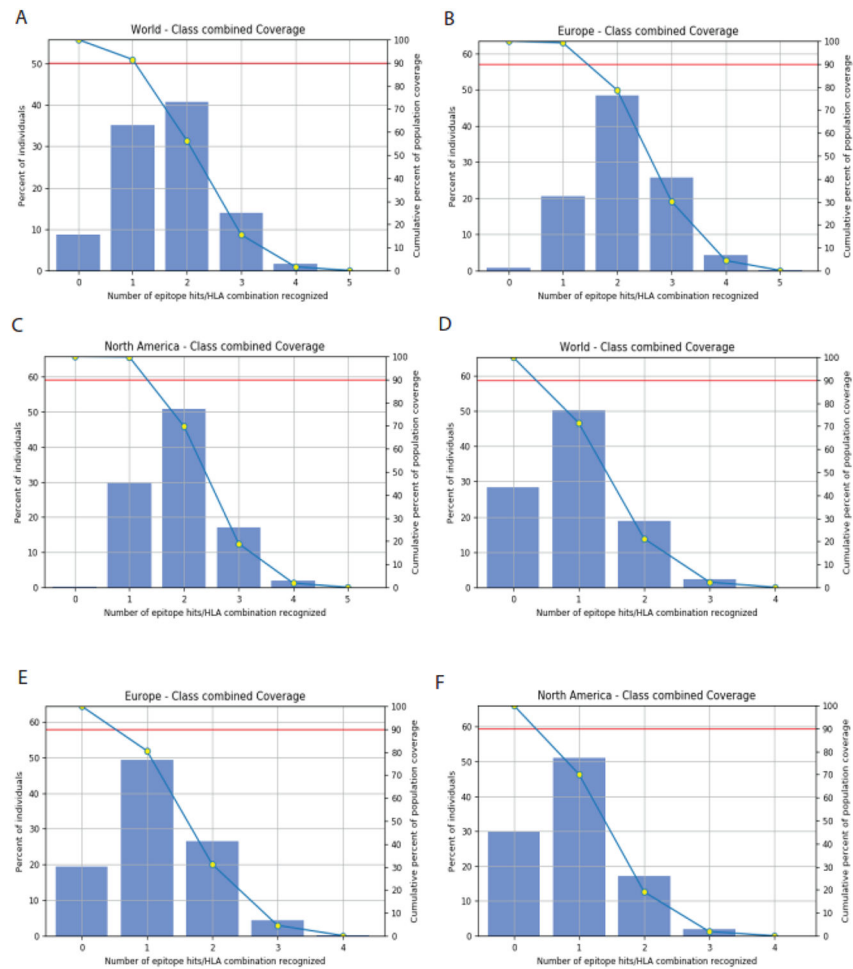
Figure 1.
Population coverage of CA-125 mRNA vaccine in breast cancer patients with CA-125 neoantigens. The combination of T helper cell and cytotoxic CD8+ T cell epitopes covered 91.39% breast cancer patients with CA-125 neoantigens worldwide (A), 99.22% in Europe (B), and 99.78% in North America (C). The selected cytotoxic CD8+ T cell epitopes only covered 71.52% breast cancer patients with CA-125 neoantigens worldwide (D), 80.58% in Europe (E), and 70.16% in North America (F).
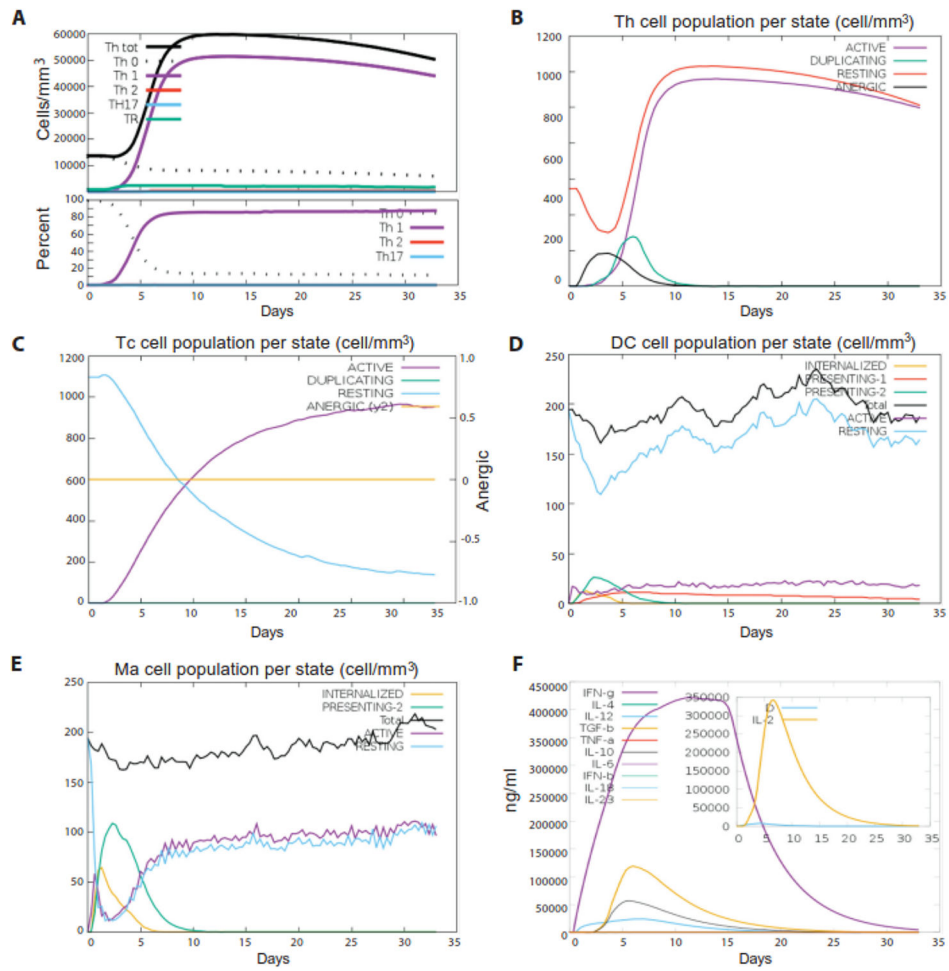
Figure 2.
In silico simulation of immune response to the mRNA vaccine of CA-125 neoantigens in breast cancer patients. After one dose of the mRNA vaccine, the change of T helper cell population (A), T helper cell population per state (B), cytotoxic T cell population per state (C), dendritic cell population per state (D), macrophage population per state (E), and cytokines and interleukins were predicted over the period of 30 days.

Figure 3.
In silico simulation of immune response to the mRNA vaccine of CA-125 neoantigens in ovarian cancer patients. After one dose of the mRNA vaccine, the change of T helper cell population (A), T helper cell population per state (B), cytotoxic T cell population per state (C), dendritic cell population per state (D), macrophage population per state (E), and cytokines and interleukins were predicted over the period of 30 days.
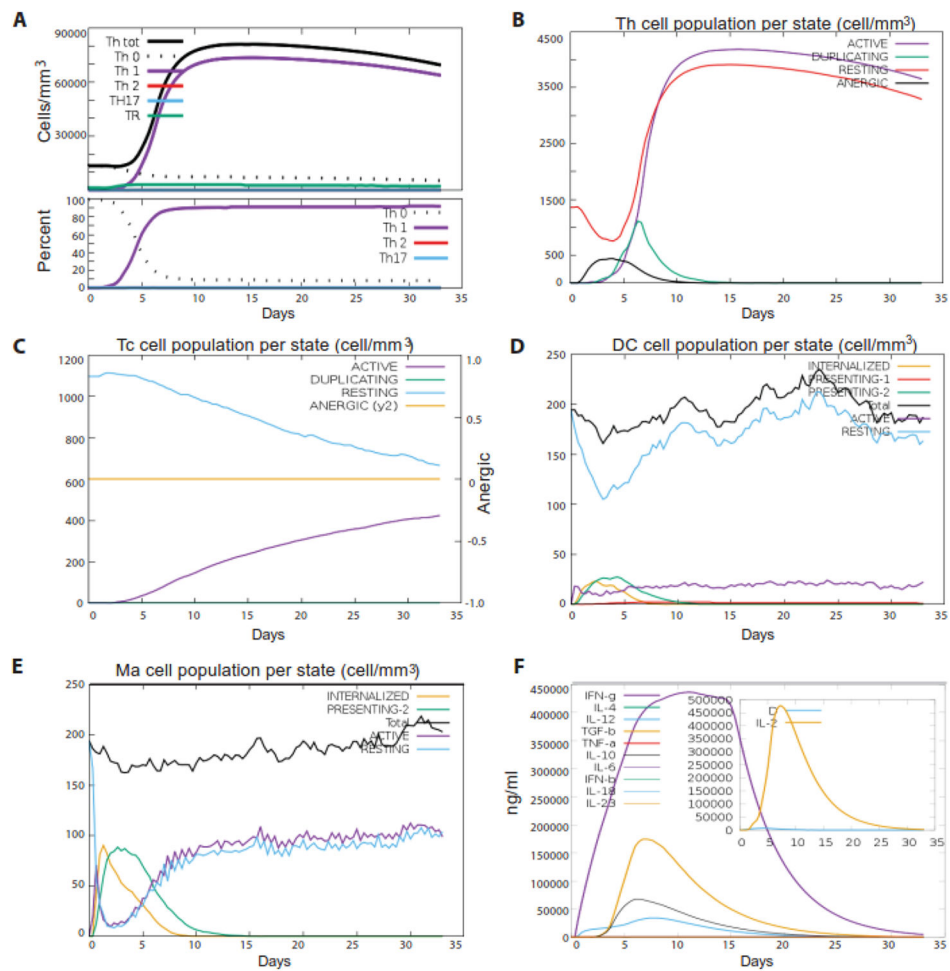
Table 1.

Predicted cytotoxic T cell epitopes, antigenicity, allergenicity and toxin of CA-125 neoantigens in breast cancer

Somatic mutation	Mutation position	MHC-I genotype	Wild-type sequence	Affinity (nM)	Mutation sequence	Affinity (nM)	Toxin prediction	Allertop prediction	Vaxijen antigenicity
L8886V	8	B*51:01	SPLRVTSL	2290.04	SPLRVTSV	145.75	non-toxin	allergen	No
S6253L	9	C*12:03	TSSLVSVTS	43310.77	TSSLVSVTL	147.09	non-toxin	allergen	No
S8117F	9	C*07:01	SRIQTEPTS	44976.52	SRIQTEPTF	56.15	non-toxin	allergen	No
P3928T	10	A*01:01	TSSPSWKSSPY	2126.77	TSSPSWKSSTY	76.04	non-toxin	allergen	No
P1758T	1	B*41:02	PDVEFIGGSTF	19824.77	TDVEFIGGSTF	395.16	non-toxin	allergen	No
T5613I	3	C*07:02	SRTPGDVSW	557.15	SRIPGDVSW	83.71	non-toxin	allergen	No
S5371F	9	B*53:01	LPVTALPTS	37238.62	LPVTALPTF	3.05	non-toxin	none	No
S4332Y	1	C*05:01	SSGDATTHV	4575.18	YSGDATTHV	35.09	non-toxin	allergen	antigen
F5552L	2	A*03:01	LFTSPIMTK	551.96	LLTSPIMTK	2.4	non-toxin	none	No
S8053F	5	C*15:02	KTHPSSNRTV	1707.33	KTHPFSNRTV	478.91	non-toxin	allergen	No
S5734Y	9	A*26:01	SISGHESQS	49786.23	SISGHESQY	276.11	non-toxin	allergen	antigen
Q13653E	2	B*49:01	MQHPGSRKF	3877.04	MEHPGSRKF	41.03	non-toxin	allergen	No
S4332Y	11	B*44:02	TETSTVITHVS	49582.49	TETSTVITHVY	198.75	non-toxin	allergen	No
T10537M	9	C*08:02	YVFPDVPET	15645.01	YVFPDVPEM	27.77	non-toxin	allergen	antigen
S8053F	1	C*15:02	SSNRTVTDV	2290.17	FSNRTVTDV	318.14	non-toxin	none	No
L8886V	2	A*34:02	SLFTPVMMKT	5030.96	SVFTPVMMKT	210.61	non-toxin	none	No
S5371F	11	B*53:01	SPLPVTALPTS	49058.99	SPLPVTALPTF	415.02	non-toxin	none	No
S2558L	9	C*17:01	VVTGSSATS	47423.84	VVTGSSATL	495.21	non-toxin	none	antigen
R13875K	4	A*02:05	GLDREQLYL	973.37	GLDKEQLYL	264.86	non-toxin	none	No
E9913K	9	A*11:01	ATTEVSMTE	35417.17	ATTEVSMTK	1.62	non-toxin	allergen	No
V10255L	2	A*02:01	SVTESTHHL	6240.33	SLTESTHHL	3.01	non-toxin	none	antigen
S8117F	7	B*38:01	IQTEPTSSL	1230.76	IQTEPTFSL	42.16	non-toxin	none	No
N4834Y	2	A*24:02	TNVGTTGSAF	47931.96	TYVGTTGSAF	8.06	non-toxin	none	No
A14192E	2	B*49:01	YAPQNLSI	46909.43	YEPQNLSI	477.96	non-toxin	none	antigen
E13026K	1	A*03:01	EDMRHPGSRK	22853.24	KDMRHPGSRK	37.13	non-toxin	allergen	No
S12624I	6	C*02:10	RLDPKSPGV	923.86	RLDPKIPGV	375.79	non-toxin	allergen	antigen
T2271I	3	A*30:01	KTTHSFRTI	1462.89	KTIHSFRTI	278.25	non-toxin	allergen	No
S8117F	9	B*38:01	SRIQTEPTS	47194.01	SRIQTEPTF	68.12	non-toxin	allergen	No

Somatic mutation	Mutation position	MHC-I genotype	Wild-type sequence	Affinity (nM)	Mutation sequence	Affinity (nM)	Toxin prediction	Allertop prediction	Vaxijen antigenicity
V10255L	2	C*05:01	SVTESTHHL	946.78	SLTESTHHL	117.86	non-toxin	none	antigen
T5613I	3	C*07:02	SRTPGDVSWM	5375.43	SRIPGDVSWM	468.71	non-toxin	none	No
A3879P	2	B*07:02	SAPWITEMM	41429.65	SPPWITEMM	433.01	non-toxin	allergen	antigen
S10124W	8	B*57:01	YSSVSIHS	48783.22	YSSVSIHW	55.14	non-toxin	allergen	No
N4834Y	1	C*12:02	NVGTTGSAF	4109.33	YVGTTGSAF	43.08	non-toxin	none	antigen
E9221K	10	A*03:01	AITEVTTDTE	49482.8	AITEVTTDTK	36.12	non-toxin	none	antigen
Q9633H	6	C*12:03	IPGPAQSTM	1112.28	IPGPAHSTM	482.77	non-toxin	none	antigen
K14116N	6	B*35:01	RPLFQKSSM	628.56	RPLFQNSSM	34.14	non-toxin	allergen	No
E530K	3	B*57:01	FSEPQHTQWV	7549.02	FSKPQHTQWV	122.81	non-toxin	allergen	antigen
T10537M	9	C*03:04	YVFPDVPET	1408.13	YVFPDVPEM	1.29	non-toxin	allergen	antigen
E12259D	3	A*02:01	TMESVLQGL	4436.06	TMDSVLQGL	28.76	non-toxin	allergen	antigen
E9770K	10	A*03:01	ILPGLVKTTE	49689.9	ILPGLVKTTK	435.86	non-toxin	none	No
E9913K	10	A*11:01	SAITEVSMTE	48950.3	SAITEVSMTK	12.6	non-toxin	none	antigen
A11739S	6	C*05:01	TISPGAPEM	511.87	TISPGSPEM	356.24	non-toxin	none	antigen
I6787L	9	C*16:04	TVMNKDPEI	1410.27	TVMNKDPEL	222.51	non-toxin	allergen	antigen
E530K	5	B*57:01	QQFSEPQHTQW	2028.8	QQFSKPQHTQW	24.86	non-toxin	allergen	antigen
S2558L	9	C*12:03	VVTGSSATS	43906.69	VVTGSSATL	52.1	non-toxin	none	antigen
S8053F	3	B*51:01	HPSSNRTV	2231.51	HPFSNRTV	11.18	non-toxin	allergen	No
E9770K	1	A*03:01	EVLDTSSEPK	29096.65	KVLDTSSEPK	10.99	non-toxin	none	antigen
E9221K	10	A*11:01	AITEVTTDTE	49461.93	AITEVTTDTK	29.04	non-toxin	none	antigen
L7045I	1	A*30:01	LTLDTSTTK	1612.02	ITLDTSTTK	418.7	non-toxin	allergen	antigen
D4025N	5	B*07:02	SPYMDTSST	681.99	SPYMNTSST	178.99	non-toxin	allergen	No
S2558L	5	C*12:03	SSATSEASL	967.47	SSATLEASL	479.83	non-toxin	allergen	No

Table 2.

Epitope sequences and their corresponding MHC-I/II binding alleles for the assembly of mRNA vaccine against CA-125 neoantigen in breast and ovarian cancer

Epitope Type	Peptide Sequence	MHC I / II binding alleles			
T helper cell epitope					
	DLPIGINITRFQTLL	HLA-DPA1*01:03	HLA-DPA1*02:01	HLA-DRB3*02:02	HLA-DRB4*01:01
		HLA-DPB1*04:01	HLA-DPB1*01:01	HLA-DRB1*04:02	
CD8+ T cell neoantigen epitope for breast cancer					
	VVTGSSATL	HLA-A*68:02	HLA-B*07:02	HLA-A*02:06	HLA-A*32:01
		HLA-A*02:03	HLA-C*12:03		
	SLTESTHHL	HLA-A*02:01	HLA-A*02:03	HLA-A*02:06	HLA-A*32:01
		HLA-B*15:01	HLA-A*24:02	HLA-A*23:01	HLA-A*26:01
		HLA-A*68:02	HLA-B*08:01	HLA-A*30:02	HLA-C*05:01
	YVGTTGSAF	HLA-B*15:01	HLA-B*35:01	HLA-A*26:01	HLA-B*53:01
		HLA-A*24:02	HLA-A*23:01	HLA-B*07:02	HLA-C*12:02
	IPGPAHSTM	HLA-B*07:02	HLA-B*35:01	HLA-B*53:01	HLA-B*51:01
		HLA-B*08:01	HLA-C*12:03		
	SATTEVSMTK	HLA-A*11:01	HLA-A*03:01	HLA-A*30:01	HLA-A*68:01
		HLA-A*32:01	HLA-A*01:01	HLA-A*11:01	HLA-A*68:01
		HLA-A*30:01	HLA-A*31:01	HLA-A*03:01	
	KVLDTSSEPK	HLA-A*03:01	HLA-A*11:01	HLA-A*30:01	HLA-A*11:01
		HLA-A*03:01			
CD8+ T cell neoantigen epitope for ovarian cancer					
	GAATGMNAI	HLA-C*12:03			
	RRNPSFGTLY	HLA-A*30:02	HLA-A*01:01	HLA-A*26:01	HLA-B*15:01
		HLA-C*07:01			
	GTSSSGHESTY	HLA-A*01:01	HLA-A*30:02	HLA-A*26:01	HLA-A*11:01
		HLA-A*32:01	HLA-A*53:01	HLA-B*15:01	HLA-B*35:01
		HLA-B*58:01	HLA-B*57:01	HLA-B*35:01	

Table 3.

Physio-chemical features of the putative synthesized protein of mRNA vaccine and optimized mRNA properties

Feature	Property for breast cancer	property for ovarian cancer
Number of amino acid	550	510
Molecular weight	60712.87	57150.79
Chemical formula	$C_{2679}H_{4208}N_{752}O_{812}S_{24}$	$C_{2517}H_{3950}N_{718}O_{759}S_{23}$
Theoretical pI	8.64	8.82
Total number of atoms	8475	7967
Total number of negatively charged residues (Asp + Glu)	51	48
Total number of positively charged residues (Arg + Lys)	58	57
Estimated half-life (in vitro mammalian reticulocytes)	30 hours	30 hours
Aliphatic index	77.35	76.16
Instability index (II)	48.43	51.52
Grand average of hydropathicity (GRAVY)	−0.349	−0.412
mRNA nucleotide length	1.65 kb	1.545 kb
GC content	66.66%	66.54
CAI	0.96	0.96